

absorption edges are the same order of magnitude⁹ as the exchange constant between the conduction electrons and the local magnetic moments. In CdCr_2Se_4 , the red shift is not observed in the photoluminescence spectra because the exchange constant is very small compared with the total blue shift of the fundamental gap.

Evidence is presented from the photoluminescence spectra for the splitting of s -conduction band in the ferromagnetic semiconductor CdCr_2Se_4 . The recent theory developed by Noltling and Olés was used to obtain the exchange energy constant of 2.3 meV between the s -conduction electrons and the Cr ions spins.

This work was supported by the U. S. Air Force Office of Scientific Research under Grant No. 80-0079. We thank Dr. W. J. Miniscalco for the samples and the helpful discussions.

¹G. Busch, B. Magyar, and P. Wachter, *Phys. Lett.* **23**, 438 (1966).

²H. W. Lehmann, *Phys. Rev.* **163**, B488 (1967).

³W. Noltling, *Phys. Status Solidi (b)* **96**, 11 (1979).

⁴T. Oguchi, T. Kambara, and K. I. Gondaira, *Phys. Rev. B* **22**, 872 (1980).

⁵F. Rys, J. S. Helman, and W. Battensperger, *Phys.*

Konden. Mater. **6**, 105 (1967).

⁶C. Haas, *Phys. Rev.* **168**, 531 (1968).

⁷K. Kubo, *J. Phys. Soc. Jpn.* **36**, 32 (1974).

⁸A. Aldea and E. Teleman, *Z. Phys. B* **37**, 135 (1980).

⁹W. Noltling and A. M. Olés, *Phys. Rev. B* **22**, 6184 (1980).

¹⁰S. S. Yao, F. Pellegrino, R. R. Alfano, W. J. Miniscalco, and A. Lempicki, *Phys. Rev. Lett.* **46**, 558 (1981).

¹¹W. J. Miniscalco, B. C. McCollum, N. G. Stoffel, and G. Margaritondo, *Phys. Rev. B* **25**, 2947 (1982).

¹²M. D. Coutinho-Filho and I. Balberg, *J. Appl. Phys.* **50**, 1920 (1979).

¹³J. Shah and R. C. C. Leite, *Phys. Rev. Lett.* **22**, 1304 (1969).

¹⁴R. F. Leheny, J. Shah, R. L. Fork, C. V. Shank, and A. Migus, *Solid State Commun.* **31**, 809 (1979).

¹⁵S. S. Yao and R. R. Alfano, to be published.

¹⁶J. F. Figueria and H. Mahr, *Phys. Rev. B* **7**, 4520 (1973).

¹⁷A. Mooradian and H. Y. Fan, *Phys. Rev.* **147**, 873 (1966).

¹⁸L. M. Roth, B. Lax, and S. Zwerdling, *Phys. Rev.* **114**, 90 (1959).

¹⁹P. K. Baltzer, P. J. Wojtowicz, M. Robbins, and E. Lopatin, *Phys. Rev.* **151**, 367 (1966).

²⁰A. Yanase and T. Kasuya, *J. Phys. Soc. Jpn.* **25**, 1025 (1968).

²¹G. Busch, P. Junod, and P. Wachter, *Phys. Lett.* **12**, 11 (1964).

Spin and Energy Analyzed Secondary Electron Emission from a Ferromagnet

J. Unguris, D. T. Pierce, A. Galejs, and R. J. Celotta

National Bureau of Standards, Washington, D.C. 20234

(Received 23 April 1982)

Measurements are presented of the energy dependence of the spin polarization of low-energy (0.5–25 eV) secondary electrons when a 500-eV primary beam is incident on an iron-based ferromagnetic glass. The polarization of the lowest-energy electrons is found to correspond to the net valence-band spin density. Possible causes for the observed decrease in polarization with increasing secondary energy are discussed. The results demonstrate a mechanism for measuring surface magnetic structure with the very high spatial resolution of scanning electron microscopy.

PACS numbers: 79.20.Hx, 75.30.+m, 75.50.Kj

We have measured the polarization of secondary electrons emitted from a ferromagnetic Fe glass target as a function of the emitted electron energy. The aim of these first measurements of spin- and energy-analyzed secondary emission from a ferromagnet was to test the hypothesis that the spin polarization of the secondary cascade is closely related to the net spin density

near the surface of the material. The results have significant implications for the study of microscopic magnetic structures including spin distributions within a domain or domain wall through the use of polarization analysis of secondary electrons in scanning electron microscopy.

When energetic primary electrons are incident on a solid, they lose energy and cause valence

electrons to be excited to unfilled conduction states by (1) direct excitation of a valence electron through the screened Coulomb interaction, (2) by Auger processes, and (3) by plasmon excitation. These excited electrons can excite still other valence electrons in a cascade process leading to the familiar low-energy peak in the energy distribution of secondary electrons. To the extent that the cascade electrons represent a uniform excitation of electrons from the valence band, the measurement of the spin polarization of these electrons should reflect the average valence-electron spin density within the solid, defined as

$$P^* = n_B/n = (n_{\uparrow} - n_{\downarrow})/(n_{\uparrow} + n_{\downarrow}). \quad (1)$$

Here $n_B = n_{\uparrow} - n_{\downarrow}$ is the difference in the number of majority (spin antiparallel to the magnetization) and minority spins per atom of alloy (i.e., the Bohr magneton number), $n = n_{\uparrow} + n_{\downarrow}$ is the total number of valence electrons per atom of alloy, and P^* is the predicted polarization.

Two studies of the polarization of secondary electrons produced by high-energy electron beams have been reported.^{1,2} One of these was from a ferromagnet where a polarization was observed but further analysis was not possible because of the poor energy resolution (500 eV) and the uncertain composition of the europium oxide film used.¹

Our ferromagnetic sample was the Fe-based glass $\text{Fe}_{81.5}\text{B}_{14.5}\text{Si}_4$ which has a room-temperature saturation magnetization³ of 176 emu/g; this corresponds to an iron magnetic moment of $1.86 \mu_B$ per Fe atom or $1.52 \mu_B$ per atom of alloy. Using $n = 7.1$ for the average number of valence electrons per atom of alloy, we can predict from Eq. (1) a valence electron polarization P^* of 21.4%.

Our measurements were carried out in an ultra-high-vacuum, magnetically shielded, surface analysis chamber.⁴ The new features for this experiment were an electron gun to provide the unpolarized primary beam, an electron-energy analyzer, and a spin-polarization analyzer. A 500-eV electron beam of typically 5–7 μA was constrained by the chamber geometry to be incident at $22^\circ \pm 2^\circ$ relative to the sample surface normal. An applied field of 50 mOe generated by a coil, illustrated schematically in Fig. 1, was sufficient to reach saturation. The stray field at the sample surface was 0.22 Oe and fell off as $e^{-z/d}$ with distance z along the surface normal, with $d = 11.5$ mm. The sample surface

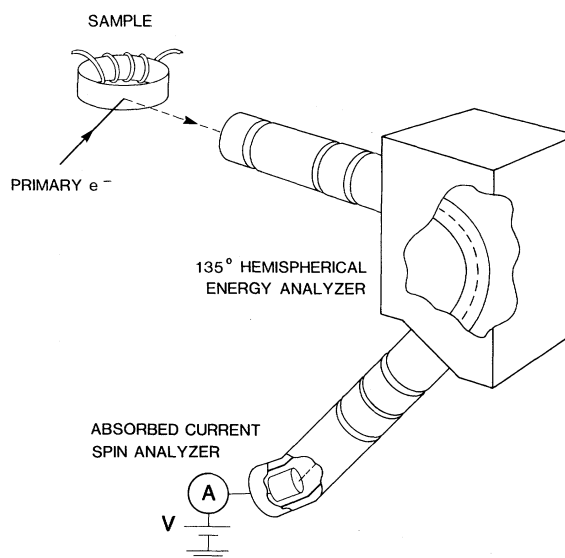


FIG. 1. Schematic of the spin- and energy-resolved secondary-electron emission experiment. The primary electron beam incident on the ferromagnetic sample generates secondary electrons which pass through the differential energy analyzer to the spin analyzer.

was prepared to give optimum hysteresis curves as measured by spin-polarized electron scattering.⁵ The preparation consisted of 500-eV Ar ion bombardment followed by annealing at 120°C for ~1 min. The Auger spectrum indicated a surface with an Fe-to-metalloid ratio 2 to 3 times higher than in the bulk and residual C contamination of 20%–30% of a monolayer which could not be removed.

The energy analyzer used was a 135° hemispherical energy analyzer and lens system⁶ operated at a resolution of 1 eV. The angular resolution of the analyzer was $\pm 4.5^\circ$ and the entrance axis of the analyzer was oriented at $33^\circ \pm 2^\circ$ from the sample surface normal in the same plane as the incident beam.

The spin analyzer⁷ follows the energy analyzer in the position usually occupied by an electron multiplier. It consists of an evaporated Au film on a Mo support with its normal at an angle of 25° to the electron beam from the energy analyzer as shown in Fig. 1. The absorbed current, A , induced in the Au film by the electrons impinging on it depends on the polarization of those electrons, an effect which is enhanced when the energy of the electrons (determined by V in Fig. 1) is near the secondary-yield crossover energy as has been described in detail previously.^{7,8} The spin analyzer measures the spin polarization along a quantization axis given by the normal to

the scattering plane formed by the beam incident on the Au film and the normal to the film. Since this quantization axis is at an angle of 33° to the magnetization of the sample the measurements are corrected for the fact that only a component of the secondary-electron polarization is measured. The entrance axis of the energy analyzer is in line with the electron beam from the GaAs spin-polarized electron source.⁹ By moving the metallic glass sample and holder to one side, it is possible to calibrate the absorbed-current spin detector directly with an electron beam of known polarization.

The results of these measurements are shown in Fig. 2. The lower part of the figure shows a curve of the number $N(E)$ of secondary electrons as a function of kinetic energy. The transmission function of the analyzer system was not studied so this curve is intended to be primarily illustrative; currents of 1–2 nA were observed at the peak of the energy distribution. The estimated uncertainty in the electron kinetic energy scale is ± 1 eV.

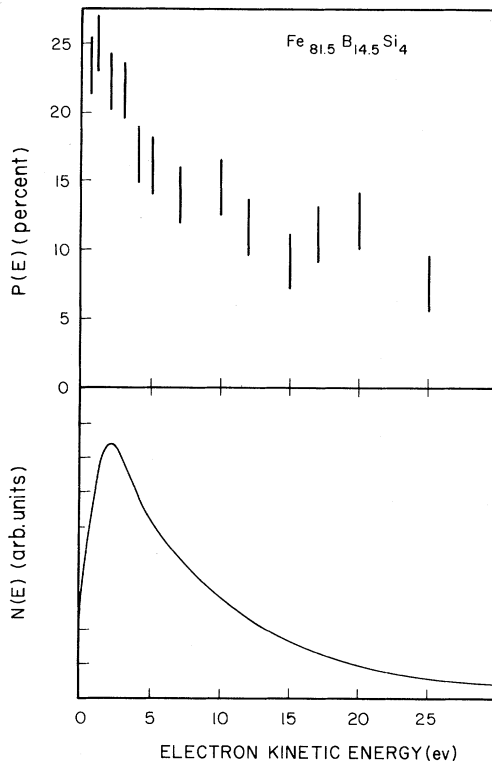


FIG. 2. Bottom: The energy distribution curve of secondary-electron emission. Top: The spin polarization of the secondary electrons as a function of kinetic energy. The experimental uncertainty is discussed in text.

Measurements were made at each secondary-electron energy by reversing the applied magnetic field to run the sample magnetization through a hysteresis cycle. This resulted in a hysteresis curve in the polarization of the secondaries. A smoothly varying background signal was also present. This spurious signal was caused by the effect of the stray magnetic field on the electron trajectories which generated a variation in the angle at which the electrons impinged on the Au film leading to a variation of the secondary-yield crossover energy and hence of the absorbed current.⁷ This stray-field behavior was simulated by a computer model in which electrons were followed from the sample to the Au film. A further test was made by exposing the sample to 600 L (1 L = 10^{-6} Torr s) O_2 . This removed the sharp hysteresis curve due to the secondary polarization. The remaining stray-field-induced signal agreed with the computer simulation. Fortunately, there was no problem in separating the sharp secondary-electron hysteresis curves from the smooth background.

The upper part of Fig. 2 shows the spin polarization of the secondary electrons $N(E)$ at each energy. The polarization of the secondaries P is defined as

$$P = [N_{\uparrow}(E) - N_{\downarrow}(E)] / [N_{\uparrow}(E) + N_{\downarrow}(E)], \quad (2)$$

where $N_{\uparrow}(E)$ [or $N_{\downarrow}(E)$] is the number of secondary electrons with spin oriented parallel [or antiparallel] to the net spin density of the ferromagnetic target. Note that factors such as the energy-analyzer transmission cancel out in Eq. (2). The error bars shown represent our estimate of the uncertainty based on the typical noise in a given measurement and the repeatability of the measurements. Additionally, there may be an overall systematic error of a few percent resulting from the detector calibration.

Within the experimental uncertainties discussed above, the low-energy value of the measured polarization P equals P^* , the net valence-electron spin density estimated in Eq. (1). The value of P which is in the range 20%–25% at low energies decreases above 3 eV and levels out to a value of approximately 10% above 10 eV. This energy dependence of the secondary-electron spin polarization is not yet understood but we can rule out several mechanisms. Depolarization of the electrons in the emission process is unlikely and has been previously observed in emission experiments in just two cases,^{10,11} neither of which is applicable here. The energy

variation of the net spin density through the valence band might be looked to as a source of energy dependence of the secondary polarization. However, Willis, Fitton, and Painter¹² have calculated the secondary-electron emission in the "random- k " or density-of-states approximation applicable to our ferromagnetic glass. The valence density of states enters the expression for the secondary current in a convolution of one-electron densities of states that would smear out any energy dependence of the net spin density. Recent energy- and angle-resolved measurements of secondary-electron emission from single crystals^{13,14} have disclosed structure on the cascade background which can be related to the electronic band structure of unfilled states above the vacuum level. Our amorphous sample exhibits no angle-dependent structure due to these states, but a spin dependence in the final density of states could be responsible for the observed energy dependence. Cluster calculations^{15,16} show, however, that a good approximation to the glass density of states can, for this Fe-based glass, be obtained from Fe band-structure calculations,¹⁷ where no spin dependence of these states is found.

The most likely cause of the energy dependence of the spin polarization of the secondaries, in our view, is the energy dependence of the secondary-electron escape depth, which is a few inelastic mean free path lengths.¹⁸ This can cause a polarization energy dependence if the spin density at the surface is different from that in the interior of the sample. Secondary electrons with 0 to 1 eV of kinetic energy have mean free paths 3–5 times as long¹⁹ as electrons with 5 to 10 eV of kinetic energy. Thus the higher-energy secondaries are much more sensitive either to an intrinsic decrease in the magnetization at the surface or to contamination at the surface which decreases the magnetization or acts as a source of unpolarized secondaries. Further studies will be required to determine if the mean-free-path mechanism is entirely responsible for the energy dependence observed here.

If the polarization of the secondaries is measured in a scanning electron microscope, then the magnitude and direction of the spin density at the specimen surface can be obtained with very high spatial resolution. Such an instrument²⁰ would have many technical applications. Unlike magnetic image-contrast techniques relying on the Lorentz force due to either fringing fields at domain walls or internal sample fields, this

spin-dependent "contrast" can be obtained in addition to but independently from the usual topological image contrast provided by the secondary electrons.

In conclusion, we have presented the first spin- and energy-resolved measurements of secondary-electron emission from a ferromagnet. We have shown that the spin polarization of the lowest-energy cascade electrons can be understood in terms of the average net spin density of the valence electrons. Further refinements of the methods reported here will allow measurements, analogous to those of Willis and Christensen¹³ for W, emphasizing additional structure on the cascade related to the single-particle density of unfilled states, which for a ferromagnetic crystal like Gd would have a rich spin dependence.

We wish to thank C. J. Powell, D. R. Penn, and S. M. Girvin for helpful discussions and F. E. Luborsky for supplying the ferromagnetic glass sample. This work was supported in part by the U. S. Office of Naval Research. One of us (J.U.) is the recipient of a National Bureau of Standards–National Research Council Postdoctoral Fellowship.

¹G. Chrobok and M. Hormann, *Phys. Lett.* **57A**, 257 (1976).

²G. Ravano and M. Erbudak, *Europhys. Conf. Abst.* **6A**, 310 (1982), and to be published; G. Ravano, M. Erbudak, and H. C. Siegmann, to be published.

³F. E. Luborsky, J. J. Becker, J. L. Walter, and H. H. Liebermann, *IEEE Trans. Magn.* **15**, 1146 (1979).

⁴D. T. Pierce and R. J. Celotta, *Adv. Electron. Electron Phys.* **56**, 219 (1981).

⁵J. Unguris, D. T. Pierce, and R. J. Celotta, to be published.

⁶C. E. Kuyatt and E. W. Plummer, *Rev. Sci. Instrum.* **43**, 108 (1972).

⁷D. T. Pierce, S. M. Girvin, J. Unguris, and R. J. Celotta, *Rev. Sci. Instrum.* **52**, 1437 (1981).

⁸M. Erbudak and G. Ravano, *J. Appl. Phys.* **52**, 5032 (1981).

⁹D. T. Pierce, R. J. Celotta, G.-C. Wang, W. N. Unertl, A. Galejs, C. E. Kuyatt, and S. R. Mielczarek, *Rev. Sci. Instrum.* **51**, 478 (1980).

¹⁰K. Sattler and H. C. Siegmann, *Phys. Rev. Lett.* **29**, 1565 (1972); M. Campagna, K. Sattler, and H. C. Siegmann, in *Magnetism and Magnetic Materials—1973*, edited by J. J. Rhyne, AIP Conference Proceedings No. 18 (American Institute of Physics, New York, 1974), p. 1388.

¹¹M. Erbudak and B. Reihl, *Appl. Phys. Lett.* **33**, 584 (1978).

¹²R. F. Willis, B. Fitton, and G. S. Painter, *Phys. Rev. B* **9**, 1926 (1974).

¹³R. F. Willis and N. E. Christensen, Phys. Rev. B **18**, 5140 (1978).

¹⁴P. E. Best, Phys. Rev. B **14**, 606 (1976).

¹⁵R. P. Messmer, Phys. Rev. B **23**, 1616 (1981).

¹⁶C. Y. Yang, K. H. Johnson, D. R. Salahub, J. Kaspar, and R. P. Messmer, Phys. Rev. B **24**, 5673 (1981).

¹⁷J. Callaway and C. S. Wang, Phys. Rev. B **16**,

2095 (1977).

¹⁸T. Koshikawa and R. Shimizu, J. Phys. D **7**, 1303 (1974).

¹⁹M. P. Seah and W. A. Dench, Surf. Interface Anal. **1**, 2 (1979).

²⁰T. H. DiStefano, IBM Tech. Disc. Bull. **20**, 4212 (1978).

Vibrational and Rotational Energy Distribution of NO Scattered from the Pt(111) Crystal Surface: Detection by Two-Photon Ionization

M. Asscher, W. L. Guthrie, T.-H. Lin, and G. A. Somorjai

Materials and Molecular Research Division, Lawrence Berkeley Laboratory, Department of Chemistry, University of California, Berkeley, California 94720

(Received 22 March 1982)

The vibrational and rotational state distributions of a supersonic nitric oxide beam, scattered from a Pt(111) single crystal surface, were investigated. A two-photon ionization technique was applied to monitor the internal energy content of the scattered molecules. Vibrational distributions were found to be colder than that corresponding to the crystal temperature between 450–1100 K. Rotational temperatures were also found to be colder than expected for thermal equilibrium with the platinum surface.

PACS numbers: 79.20.Rf, 33.80.Kn

The dynamics of gas-molecule-surface interactions has received increasing experimental and theoretical attention in recent years. Laser-induced fluorescence or bolometer detection techniques were used to investigate the excitation of rotational states in NO molecules scattered from metal surfaces,¹⁻⁴ and of CO and HF molecules scattered from the LiF surface.^{5,6} Atomic recombination of nitrogen on an iron foil produces vibrationally hot N₂ molecules, as determined by high-energy electron beam excitation.⁷ Theoretical studies have attempted to predict the rotational excitation of diatomic molecules upon scattering from smooth solid surfaces.⁸⁻¹⁰

We report the direct observation of vibrationally excited NO molecules scattered from a clean Pt(111) crystal surface using a two-photon ionization (TPI) technique. The vibrational and rotational energy distributions were determined as a function of crystal temperature and angle of scattering. We found that the population of excited vibrational ($v''=1$) and rotational states is less than the population when thermal equilibrium between the crystal and the desorbed NO is assumed.

The molecular-beam-surface scattering apparatus was described elsewhere¹¹; the modified version used in this laser ionization study will be described in detail in a future publication.¹² The scheme of the scattering and ionization detection

is shown in Fig. 1. Briefly, a supersonic molecular beam from a differentially pumped source impinges upon a single-crystal sample, located in the ultrahigh vacuum scattering chamber. The beam characteristics are 100 meV incident kinetic

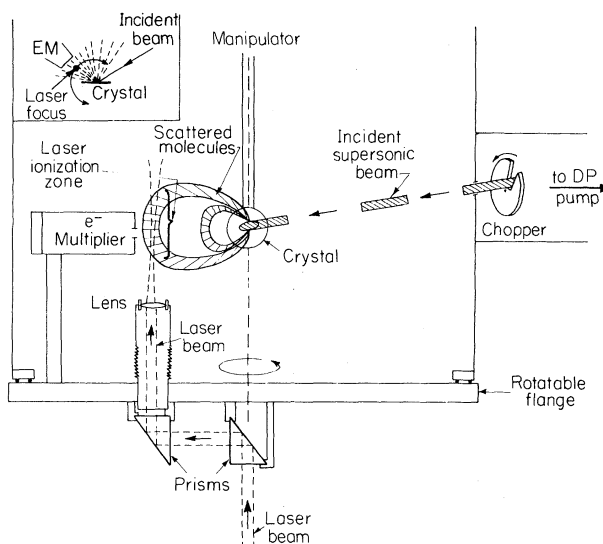


FIG. 1. Schematic of the molecular-beam-surface scattering experiment with laser-induced two-photon ionization as a probe for internal-state energy distributions.